Toughened Single-lap Joints by Composite Bondline of Adhesive and Double-sided Tape

Kosuke Takahashi[a]*, Zhantong Sun[b], Takuma Kikuzawa[b], Kounosuke Shimamura[b], Sourabh Jagrat[b], Nao Fujimura[a], and Takashi Nakamura[a]

[a]*Division of Mechanical and Aerospace Engineering, Faculty of Engineering, Hokkaido University, Kita 13, Nishi 8, Kita-ku, Sapporo, Hokkaido 060-8628, Japan*

[b]*Division of Mechanical and Space Engineering, Graduate School of Engineering, Hokkaido University, Kita 13, Nishi 8, Kita-ku, Sapporo, Hokkaido 060-8628, Japan*

ktakahashi@eng.hokudai.ac.jp

Toughened Single-lap Joints by Composite Bondline of Adhesive and Double-sided Tape

This study proposes the novel manufacturing method of adhesively bonded joint with double-sided tapes by following the concept of bi-adhesive bondline. The stress concentration at the ends of the bondline for a single-lap joint can be suppressed by utilizing flexibility of the double-sided tapes. The double-sided tapes also make it easy to control the bondline thickness and to hold the adherends with their stickiness until complete cure. A tensile-shear test of the aluminum / acrylic joint verified that replacing both ends of the 30 mm bondline by the 3 mm double-sided tape improved the maximum load by more than 20%. The observation on the bonded area through the transparent acrylic plate revealed the suppression of the debonding initiation. On the other hand, the aluminum / aluminum joint did not show the significant increase of the maximum load, but suppressed the unstable interfacial debonding. The strain distribution obtained by digital image correlation method proved that the double-sided tape has the same effect of compressive strain generated in the flexible adhesive in bi-adhesive bondline.

Keywords: adhesive bonding, double-sided tape, single-lap joint, stress concentration

1. Introduction

The demand for adhesive bonding has been increasing in various industrial fields such as automobiles and aircrafts, which require numerous parts and assembly processes [1,2]. Adhesive bonding can improve the structural performance by selecting suitable materials in the right place and reduce the weight of bolts or rivets used in the mechanical joints. However, the adhesive bonding has a primary issue in the reliability because the quality of the adhesive joint strongly depends on the manufacturing process. To reduce the variation of quality in the adhesive joints, the characterization and the development of adhesive materials [3–5], the surface treatment of the adherends [6, 7], and the durability against hygrothermal environments [8, 9] has been intensively investigated. Even if highly reliable materials are prepared based on these achievements, the design of the adhesive bonding is another concern. A single-lap joints is the simplest design to replace the bolts or rivets, but it causes the stress concentration at the end of the bondline owing to the discontinuity of the material, as shown in Fig. 1 [10,11]. Because the stress concentration is sensitive to various parameters such as the length and the thickness of the bondline [12–16], it is necessary to apply the suitable joint design for individual applications. Practically, the adhesive bonding is used together with mechanical joints of bolts or rivets to enhance the structural safety against rapid debonding propagation [17–19].

Various approaches have been proposed to suppress the stress concentration in the single-lap joint. The scarf joint is effective by inclining the adherend to reduce the discontinuity [20–22], but they are difficult to apply to thin adherends. The bi-adhesive bondline, which applies a flexible adhesive at both ends of the bondline also relieves the stress concentration, as shown in Fig. 2 [23–26]. The bi-adhesive bondline is a promising joint technology, which is effective regardless of the adherend thickness, but the manufacturing process becomes complicated. It is necessary to distribute different adhesive materials on the same bondline with the precise control of the bondline thickness. Mixing glass beads in uncured adhesive is a way to adjust the layer thickness based on their diameters, but it might cause initial defects in the joint. To improve the reliability and manufacturability of adhesively bonded joint, the layer thickness should be easily and uniformly adjusted without adverse effects on the joint strength.

This study proposes to use double-sided tapes for simple adjustment of the bondline thickness, as well as the suppression of stress concentration of a single-lap joint. Double-sided tapes have been widely used in industries particularly in electronics by utilizing their instant adhesion for efficient manufacturing process and flexibility for releasing thermal residual stress [27-28]. They are attached at the end of the bondline instead of flexible adhesive for the bi-adhesive bondline. A uniform thickness of the adhesive layer can be automatically achieved using the thickness of the double-sided tape. In addition, the manufacturing process becomes drastically easier because the stickiness of the double-sided tape can support to fix the adherends during the curing process. The effectiveness of the proposed bonding method was investigated using a single-lap joint of aluminum and acrylic plates by varying the tape lengths. Their joint strengths were compared with a detailed observation of the fracture process on the bonded area by utilizing the transparency of the acrylic plate. Another single-lap joint of two aluminum plates was also prepared to show the effectiveness under the adhesive failure without causing fracture of the adherend plates. The strain distribution along the bondline was analysed using a digital image correlation (DIC) method to validate that the double-sided tape can be alternative for the flexible adhesive in bi-adhesive bondline.

2. Experimental method

2.1 Sample preparation

In this study, 5052 aluminium alloy plates and acrylic plates were used as adherends for the single-lap joint. The mechanical properties of the plates are summarized in Table 1. Both adherends were cut from the 3 mm thick plates to a length of 100 mm with a width of 25 mm. The surface of the plates was then prepared by following ISO 17212:2012; it was wet-polished using an automatic rotary polishing machine with # 240 sandpaper, subsequently degreased with ethanol, and dried in a vacuum constant-temperature dryer DRV320DB (Advantec Toyo Kaisha, Ltd.) for 24 hours. The aluminum and acrylic plates were then covered with Teflon tape along the end of the bond area to prevent excess adhesive from flowing out of the bondline and affecting the joint strength.

A two-component mixed epoxy adhesive DP 110 CLE (3M Corp.) was used for the bonding. When the epoxy adhesive was applied to the plates, a fixture and spacer, which were made of Teflon plates, were used to maintain the bondline thickness to be 0.4 mm for the single-lap joint of aluminium and acrylic plates. Because it was prepared for directly observing the bonded area through the transparent acrylic plate, the bondline thickness was designed to be sufficiently thin to be focused on by a CCD camera. The bondline length was preliminary examined and determined to be 30 mm so that the joint was strong enough to cause the fracture of acrylic plate, while the interfacial separation occurred when the bondline was 20 mm. Another single-lap joint of two aluminum plates was prepared for measuring the strain using DIC method. The bondline thickness was thicker, 0.8 mm, to have sufficient area for the strain analysis. The sample of only adhesive along the bondline is referred to as "bondline_30 mm". The dimensions of the single-lap joints of aluminum / acrylic plates and two aluminum plates were shown in Fig. 3 (a) and (b) respectively.

In addition to only adhesive bondline, the acrylic tape G-304 (3M Japan Corp.) was used to supress the stress concentration. This tape was designed to have high peeling strength and environmental toughness for fixing displays and signboards outside, whose adhesion strength and service temperature is 1500 N/m and -30 ~ 200 °C, respectively. Three types of the bondlines were prepared by replacing both ends of the bondline with the tape length of 1, 3, and 5 mm, represented by "bondline_1-28-1 mm", "bondline_3-24-3 mm sample", and "bondline_5-20-5 mm", respectively. The tapes were attached at both ends of the bondline before painting the epoxy adhesive such that the bondline thickness can be controlled. Therefore, the insertion of a Teflon spacer, which was required for only adhesive bondline, was not necessary. In addition, the stickiness of the tapes helps to temporarily fix the plates during the curing process of the adhesive.

All samples were placed on a hotplate at a temperature of 40 °C for 24 hours during the curing process. A paper cup filled with 100 g of water was used as a weight to provide a constant pressure of 1.3 kPa to all samples. After curing, the side surface of the specimen was polished with # 400 sandpaper carefully to remove the squeezed excess adhesive. The manufactured single-lap joints of aluminum and acrylic plates are shown in Fig. 4. The double-sided tapes are the grey area at both ends of the bondline, which can be seen through the transparent acrylic plate. Although an excess amount of adhesive slightly overflowed from a bondline, it kept remained to avoid damaging the bondline. Because Teflon tapes were attached along both ends of the bondline, there was no contact between the overflow adhesive and the plates. The average bondline thickness of all the joints, measured from 3 samples of each joint configuration, are shown in Fig. 5 (a) for the aluminum and acrylic plates and Fig. 5 (b) for two aluminum plates. The bondline with double-sided tapes are slightly thinner than the thickness of the original double-sided tape, which is 0.4 mm for the joint of aluminum and acrylic plates and 0.8 mm for two aluminum plates, owing to the applied weight during the curing process. The bondline thickness of only adhesive was thicker than the Teflon spacer due to its warp. Further improvement is required for the mold and the spacer for only adhesive joint, while the thickness can be easily and accurately controlled using the double-sided tape once it is related to the weight during the cure.

2.2 Tensile-shear test

A tensile-shear test was performed using a Instron 5982 testing machine at a tensile speed of 2 mm/min. The test was performed at a room temperature of 25 ± 1°C. Before the test, a speckle pattern was painted on the side surface of the bondline using an airbrush for all the joints of two aluminum plates. First, the side surface was sufficiently sprayed to be flat white as a base to minimize the error in the image information. Next, an identifiable pattern was obtained by evenly spraying flat black. The painted area was recorded using a CCD camera Grasshopper3 GS3-U3-51S5M (Teledyne FLIR LLC) with a 35 mm lens and analysed using Vic-2D (Correlated Solutions, Inc.). The image taken by this camera has 5M (2448 ×2048) pixels at the frame rate of 20 fps. The subset size was determined to be 39 pixels which corresponds to 1/4 of the bondline thickness. The step size was 7 pixels to obtain sufficiently smooth strain distribution in the analyzed area. The aluminum and acrylic joints were observed through the acrylic plate using the same camera to capture the debonding process in the bonded area.

3. Results and discussion

3.1 Joint of aluminium and acrylic plates

The load and displacement relationships obtained from all the joints of aluminum and acrylic plates are shown in Fig. 6(a). When the end of the bondline was replaced by the double-sided tape, both the maximum load and displacement increased compared to the only adhesive bondline_30 mm. The average values of the maximum load are shown in Fig. 6(b). The error bars represent the maximum and minimum values obtained from three samples with the same configuration. Among the samples with various tape lengths, the bondline_3-24-3 mm exhibited the highest load, which is higher by 20% compared to the bondline_30 mm. It implies that there is an optimum tape length because insufficient tape length cannot suppress the stress concentration, but excess tape length cannot sustain the high tensile load. Nevertheless, all the samples showed the fracture of the acrylic plates. It means that the bending stress generated by the tensile-shear test reached the flexural strength of the acrylic plate. The higher maximum loads imply the suppression of bending deformation of the acrylic plate, which could be assisted by elongation of the double-sided tape.

The images of the bonded area captured during the test were shown in Fig. 7 (a)–(d) with the acrylic plate on the left and the aluminium plate on the right, arranged in the same directions in Fig. 4. The field of view was focused on the bonded area through the acrylic plate. The first image (top) and the last image (bottom) were captured before loading and soon after the fracture, respectively. The images in the middle were captured at the circles in the Fig. 6; 2.53 N, 2.74 N, and 3.02 N for bondline_30 mm, 2.57 N, 2.88 N, and 3.17 N for bondline_1-28-1 mm, 3.16 N, 3.46 N, and 3.88 N for bondline_3-24-3 mm, and 3.08 N, 3.21 N, and 3.31 N for bondline_5-2-5 mm, respectively. In the case of bondline_30 mm (Fig. 7 (a)), the local debonding occurred at the upper-left corner, as indicated by the red arrows in the second image. It expanded gradually with increasing loading, as shown in the third and fourth images. The acrylic plate then fractured along the tip of debonding. The sample of bondline_1-28-1 mm (Fig. 7(b)) also showed the local debonding at the upper left corner, but along the boundary with the tape, as shown in the second and third images. The debonding gradually expanded along the boundary toward the lower left corner, as shown in the fourth image, followed by fracture of the acrylic plate along the tip of the debonding. On the other hand, it was difficult to detect the debonding from the bondline_3-24-3 mm, whose maximum load was the highest, because the debonded area was significantly smaller compared to the other samples (Fig. 7(c)). The debonding became finally apparent just before the fracture as shown in the second and third images. The acrylic plate fractured a few millimeters away from the observed tip of the debonding. The bondline_5-2-5 mm exhibited the similar debonding pattern to that of bondline_3-24-3 mm (Fig. 7(d)); the debonding area was tiny along the boundary of the double-sided tape, and became apparent just before the fracture as shown in the fourth image. In addition, the load at the second image when the debonding was first detected was close to that of bondline_3-24-3 mm. These results implies that the double-sided tape longer than 3 mm effectively suppressed the initiation of the debonding and delayed the fracture of the acrylic plate.

3.2 Joint of two aluminium plates

The load and displacement relationships obtained from all the joints of two aluminum plates, and the average values of the maximum load are shown in Fig. 8(a) and (b), respectively. The error bars represent the maximum and minimum values obtained from three samples with the same configuration. The increase of the maximum load by double-tapes at both ends of the bondline was less significant compared with the increase obtained from aluminium and acrylic plates. However, the load decreased gradually before the complete fracture whereas the bondline of only adhesive_30 mm caused the fracture in brittle manner. Because all the joints caused the interfacial debonding without fracture of aluminum plates, the suppression of the unstable interfacial debonding was confirmed by the double-sided tape.

The bondline of all the samples was observed from the side surface as shown in Fig. 9. The first image (top) and the last image (bottom) were captured before loading and soon after fracture, respectively. The images in the middle were captured at the circles in the Fig. 8; 4.00 N, 5.20 N, and 6.53 N for bondline_30 mm, 4.00 N, 4.76 N, and 4.18 N for bondline_1-28-1 mm, 4.00 N, 6.50 N, and 4.19 N for bondline_3-24-3 mm, and 4.00 N, 6.82 N, and 4.89 N for bondline_5-2-5 mm, respectively. The speckle pattern was used for DIC analysis in the following paragraph. No particular change was detected from only adhesive bondline _30 mm until complete fracture (Fig. 9(a)). The epoxy adhesive was continuous but separated from each root of top and bottom plates. The bondline_1-28-1 mm (Fig. 9(b)) exhibited the crack propagation from the root of the bondline indicated by the red arrow. It was detected after the slight decrease of the load at the displacement of 0.5 mm. The stable crack propagation was observed as shown in the fourth image with the gradual decrease of the load. The bondline_3-24-3 mm (Fig. 9(c)) also exhibited the crack propagation from the root of the bondline as shown in the fourth image, but the image soon after the fracture showed the separation from the tip of each plate with scission of the adhesive layer. The bondline_5-20-5 mm (Fig. 9(d)) did not cause the detectable crack from the side surface. The fracture pattern was the same as that of bondline_3-24-3 mm, whose interfacial separation occurred from each tip of the plates with scission of the adhesive layer.

The strain of the adhesive layer was obtained from the DIC method. The distributions of the shear and normal strains were compared at the same loading of 4 kN because the strain analysis at the higher load showed the error in the region of double-sided tapes. No damage was observed at 4 kN from the side surface as shown in the second images in Fig. 9(a)-(d). The contours of the strain are shown in Fig. 10 (a)–(d) for the bondline_30 mm, 1-28-1 mm, 3-24-3 mm, and 5-20-5 mm, respectively. Shear and normal strains are shown on the left and right, respectively. Compared to the bondline_30 mm, the bondline_1-28-1 mm showed the higher shear strain toward both ends on the bondline symmetrically. Their normal strains were negligibly low along the entire bondline. The bondline_3-24-3 mm and the bondline_5-20-5 mm exhibited a high shear strain along the entire bondline with higher values toward both ends. Their normal strain was high only at the region of the double-sided tape.

To interpret the strain distribution in more detail, the shear and normal strains along the middle of the adhesive layer was extracted from the left to right ends. The shear and normal strains were compared among the different tape lengths in Fig. 11(a) and (b), respectively. The horizontal axis is the location of the bondline from the left to the right ends at -15 to 15 mm. The bondline_1-28-1 mm exhibited the similar shear strain in the center of the bondline and higher strain toward both ends. Compared to these shear strains, those of the bondline_3-24-3 mm and bondline_5-20-5 mm were much higher entirely along the bondline. The minimum value at the center is 1.4%, which is even higher than the highest strain at the end of bondline_1-28-1 mm. The sample of bondline_5-20-5 mm showed the higher strain toward both ends, particularly on the double-sided tapes. It was confirmed that the change of the shear strain distribution was not proportional to the length of double-sided tapes, but it increases drastically from the tape length of 3 mm, which corresponded to the improvement of the fracture elongation shown in Fig. 8. On the other hand, the normal strain is negligibly low in the region of epoxy adhesive as shown in Fig. 11(b). The higher normal strain was observed accordingly from the longer double-sided tapes with the compressive strain in the epoxy adhesive near the boundary. The transition from tension to compression roughly corresponded to the boundary between the double-sided tape and the epoxy adhesive. The compression in the epoxy adhesive suppressed the debonding propagation and resulted in the gradual decrease of the load in Fig. 8(a). This strain distribution is very similar to that reported in the bi-adhesive joint [26], which exhibited the maximum compressive strain in the hard adhesive region when the length of the flexible adhesive is sufficiently short. Therefore, it was verified that the double-sided tape attached at both ends of the bondline has the same effect as the bi-adhesive joint.

The tensile strain along the interface of aluminum plate, which is represented in the red arrow in Fig. 9(a), was also extracted at the load of 4 kN and plotted in Fig. 12(a). The position of the tip of the aluminum plate is defined as -15 mm in the horizontal axis. The tensile strain of the aluminum plate is quite similar regardless of the length of the double-sided tapes. The maxim tensile strain at the load of 4 kN was 0.0025, which was slightly lower than the strain at the proof stress of A5052, $\varepsilon_y \approx 0.003$. The strain distribution was also extracted from the image at the maximum loading point from all the samples and shown in Fig. 12(b). The maximum strain values of 0.006, which implied plastic deformation, were similar in accordance with the similar maximum loads in Fig. 8(a). Although the maximum strains were observed near the end of bondline (x = 15 mm) in the case of the bondline_30 mm and 1-28-1 mm, those of the bondline_3-24-3 mm and 5-20-5 mm were close to the boundary with the epoxy adhesive region. Therefore, the double-sided tapes do not affect the load transfer through the bonded area at the lower loads, but changes the bending deformation of the plates toward the failure load. The effect of the double-sided tapes on the deformation of substrate plates and compressive strain in the epoxy adhesive region will be related to the suppression mechanism of debonding propagation in the future work.

4. Conclusions

In this study, the new concept of the composite bondline, which is the combined use of double-sided tapes for adhesively bonded single-lap joints, was proposed. Both ends of the 30 mm bondline were partially replaced by double-sided tapes to control the thickness of the bondline and to suppress the stress concentration. The proposed composite bondline does not require any spacers to control the thickness, but its variation of the thickness was similar to that of only adhesive bondline which required the spacers and careful alignment during the curing process.

First, the tensile-shear tests were conducted for the joint of aluminum and acrylic plates. The fracture process on the bonded area was observed through the transparent acrylic plate. The initiation of the interfacial debonding was confirmed at the higher loads by replacing the end of bondline with the double-sided tape. All the joints caused the fracture of the acrylic plate, while the tape length of 3 mm showed the highest breaking load compared with that of 1 mm and 5 mm. These results mean that the double-sided tape has an optimum length.

Second, the same tests were conducted for the joint of two aluminum plates. All the joint showed the interfacial debonding without causing the fracture of the aluminum plates. The joint of only adhesive fractured in a brittle manner, whereas the proposed composite joint showed the gradual decease of the load before the separation. The strain distribution of the adhesive layer was obtained by the digital image correlation. The normal strain is negligibly low along the adhesive although the higher strain was observed in the longer tape length. Furthermore, the compressive strain was confirmed in the epoxy adhesive near the boundary with the double-sided tape similarly to that observed in bi-adhesive bondline with the flexible adhesive. Therefore, it was proved that the double-sided tape has the equivalent effect as the flexible adhesive for the bi-adhesive bondline. Further improvement of the joint strength would be possible by utilizing the computer simulation for more detailed stress analysis and by clarifying the suppression mechanism of the debonding propagation in the proposed composite bondline.

Acknowledgement

This research was supported by the Adaptable and Seamless Technology Transfer Program through Target-driven R&D (A-STEP) from the Japan Science and Technology Agency (JST), Grant Number JPMJTM 20A6.

References

[1] Markatos DN, Tserpes KI, Rau E, Markus S, Ehrhart B, Pantelakis S. The effects of manufacturing-induced and in-service related bonding quality reduction on the mode-I fracture toughness of composite bonded joints for aeronautical use. Compos Part B Eng 2013;45:556–64.

[2] Banea MD, da Silva LFM. Adhesively bonded joints in composite materials: an overview. Proc Inst Mech Eng Part L J Mater Des Appl 2009;223:1–18.

[3] Imanaka M, Liu X, Kimoto M. Comparison of fracture behavior between acrylic and epoxy adhesives. Int J Adhes Adhes 2017;75:31–9.

[4] Ratna D, Banthia AK. Rubber toughened epoxy. Macromol Res 2004 121 2004;12:11–21.

[5] Sprenger S. Nanosilica-Toughened Epoxy Resins. Polym 2020, Vol 12, Page 1777 2020;12:1777.

[6] Saleema N, Sarkar DK, Paynter RW, Gallant D, Eskandarian M. A simple surface treatment and characterization of AA 6061 aluminum alloy surface for adhesive bonding applications. Appl Surf Sci 2012;261:742–8.

[7] Molitor P, Barron V, Young T. Surface treatment of titanium for adhesive bonding to polymer composites: a review. Int J Adhes Adhes 2001;21:129–36.

[8] Custódio J, Broughton J, Cruz H. A review of factors influencing the durability of structural bonded timber joints. Int J Adhes Adhes 2009;29:173–85.

[9] Marques EAS, Da Silva LFM, Banea MD, Carbas RJC. Adhesive Joints for Low- and High-Temperature Use: An Overview. 2014;91:556–85.

[10] Her SC. Stress analysis of adhesively-bonded lap joints. Compos Struct 1999;47:673–8.

[11] Tsai MY, Morton J. An evaluation of analytical and numerical solutions to the single-lap joint. Int J Solids Struct 1994;31:2537–63.

[12] Ayatollahi MR, Akhavan-Safar A. Failure load prediction of single lap adhesive joints based on a new linear elastic criterion. Theor Appl Fract Mech 2015;80:210–7.

[13] Davies P, Sohier L, Cognard JY, Bourmaud A, Choqueuse D, Rinnert E, Créac'hcadec R. Influence of adhesive bond line thickness on joint strength. Int J Adhes Adhes 2009;29:724–36.

[14] Campilho RDSG, Moura DC, Banea MD, da Silva LFM. Adherend thickness effect on the tensile fracture toughness of a structural adhesive using an optical data acquisition method. Int J Adhes Adhes 2014;53:15–22.

[15] Akhavan-Safar A, Ayatollahi MR, da Silva LFM. Strength prediction of adhesively bonded single lap joints with different bondline thicknesses: A critical longitudinal strain approach. Int J Solids Struct 2017;109:189–98.

[16] Stephan Marzi, Anders Biel US. On experimental methods to investigate the effect of layer thickness on the fracture behavior of adhesively bonded joints. Int J Adhes Adhes 2011;31:840–50.

[17] Kelly G. Quasi-static strength and fatigue life of hybrid (bonded/bolted) composite single-lap joints. Compos Struct 2006;72:119–29.

[18] Kweon JH, Jung JW, Kim TH, Choi JH, Kim DH. Failure of carbon composite-to-aluminum joints with combined mechanical fastening and adhesive bonding. Compos Struct 2006;75:192–8.

[19] Sadowski T, Kneć M, Golewski P. Experimental investigations and numerical modelling of steel adhesive joints reinforced by rivets. Int J Adhes Adhes 2010;30:338–46.

[20] Lang TP, Mallick PK. Effect of spew geometry on stresses in single lap adhesive joints. Int J Adhes Adhes 1998;18:167–77.

[21] Rispler AR, Tong L, Steven G, Wisnom MR. Shape optimisation of adhesive fillets. Int J Adhes Adhes 2000;20:221–31.

[22] Chen Z, Adams RD, da Silva LFM. Prediction of crack initiation and propagation of adhesive lap joints using an energy failure criterion. Eng Fract Mech 2011;78:990–1007.

[23] Boss J, Ganesh V, Lim C. Modulus grading versus geometrical grading of composite adherends in single-lap bonded joints. Compos Struct 2003;62:113–21.

[24] da Silva LFM, das Neves PJC, Adams RD, and Spelt JK. Analytical models of adhesively bonded joints—Part I: Literature survey. Int J Adhes Adhes 2009;29:319–30.

[25] Löbel T, Holzhüter D, Sinapius M, Hühne C. A hybrid bondline concept for bonded composite joints. Int J Adhes Adhes 2016;68:229–38.

[26] Ramezani F, Ayatollahi MR, Akhavan-Safar A, da Silva LFM, A comprehensive experimental study on bi-adhesive single lap joints using DIC technique, Int J Adhes Adhes 2020;102;102674

[27] Creton C. Pressure-Sensitive Adhesives: An Introductory Course, MRS Mulletin 2003;28;6;434-439

[28] Creton C, Pason E. Materials Science of Adhesives: How to Bond Things Together 2003;2003;38;6;419-423

Table 1 Mechanical properties of plates

	Elastic modulus [GPa]	0.2% proof stress [MPa]	Tensile strength [MPa]
Aluminum plate	68.0	215	260
Acrylic plate	3.27	37.7	59.1

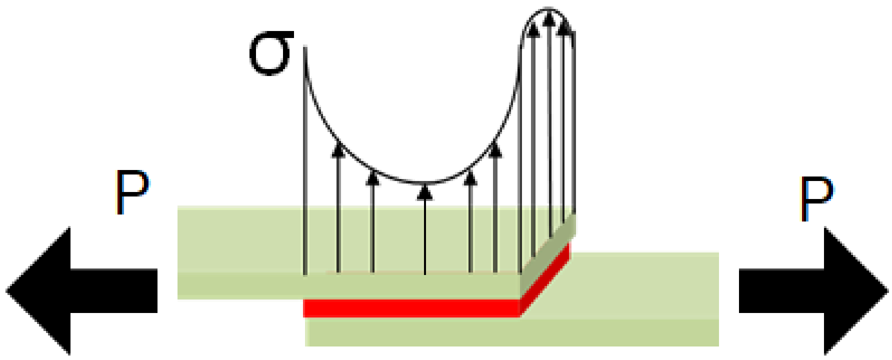

Fig. 1 Schematic image of stress concentration caused in single lap joint

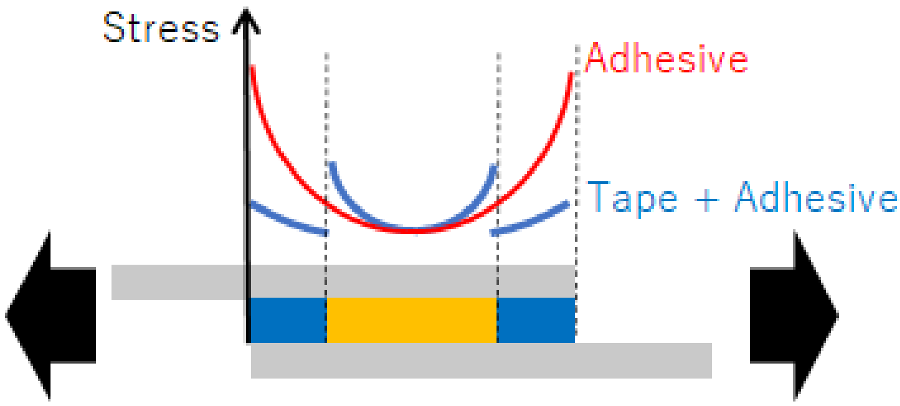

Fig. 2 Reduction of stress concentration by bi-adhesive joint

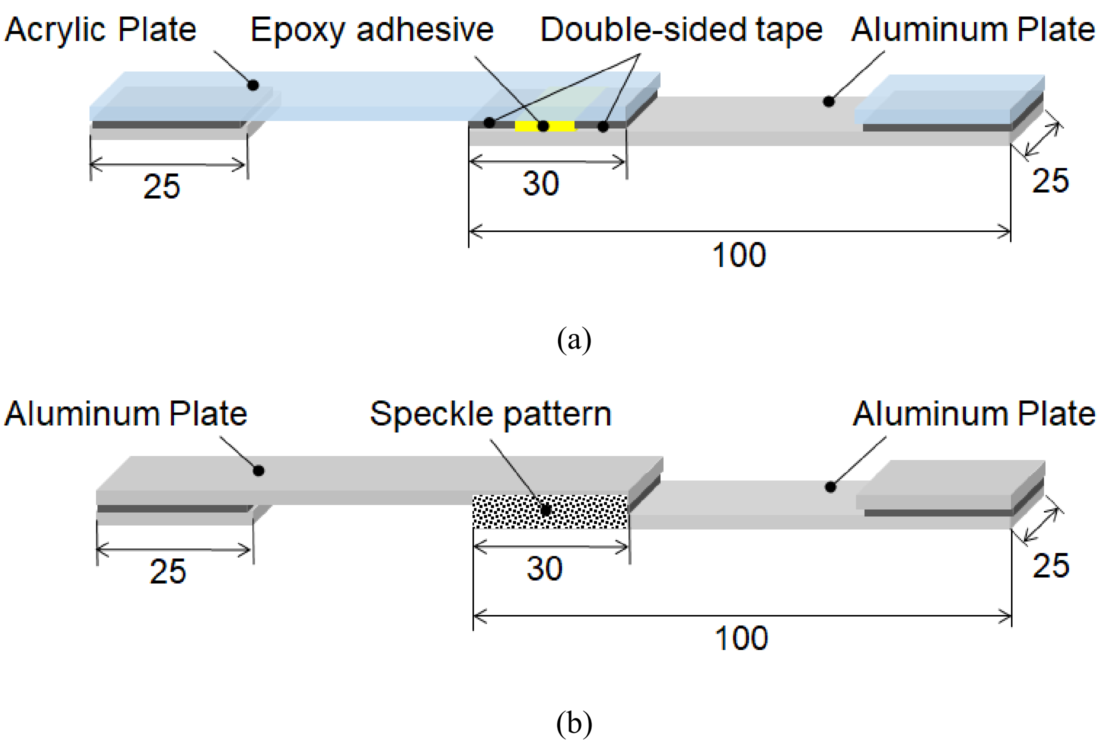

Fig. 3 Configuration of single-lap joint specimen with double-sided tapes on both ends of bond-line

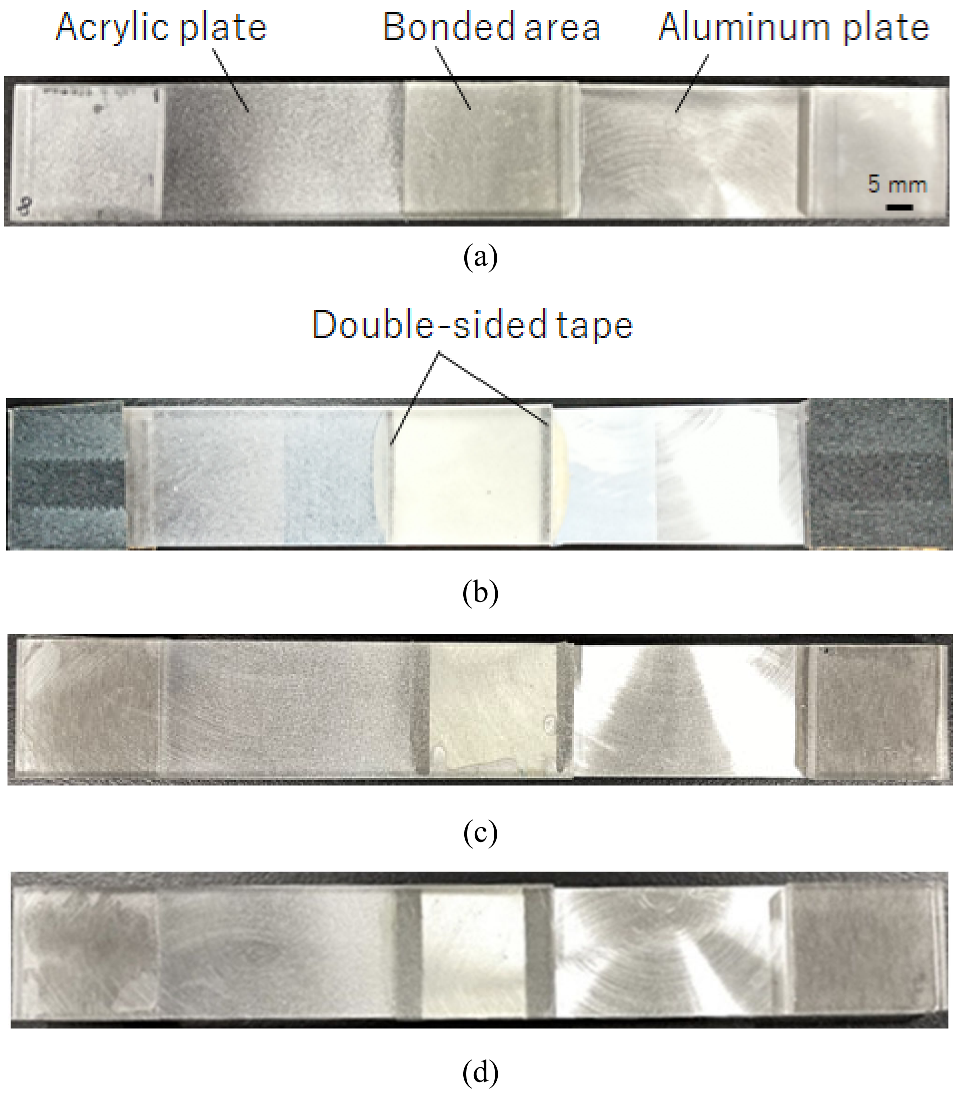

Fig. 4 Images of single-lap joint specimen with the bond-line of 30 mm (a), and the replacement of both ends by double-sided tape with 1 mm (b), 3 mm (c) and 5 mm (d)

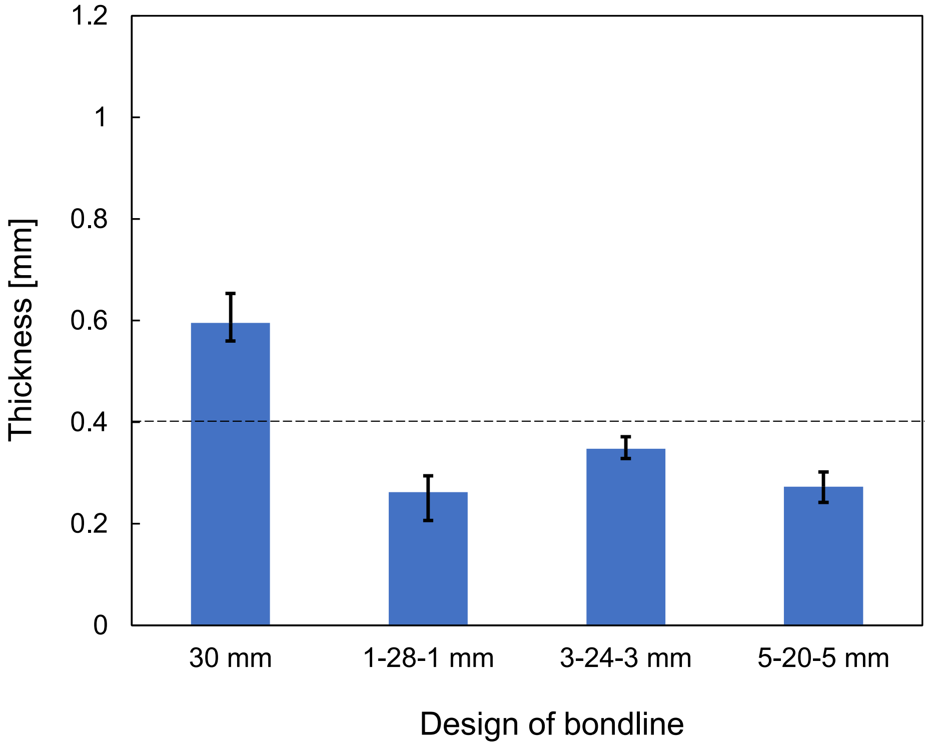

(a)

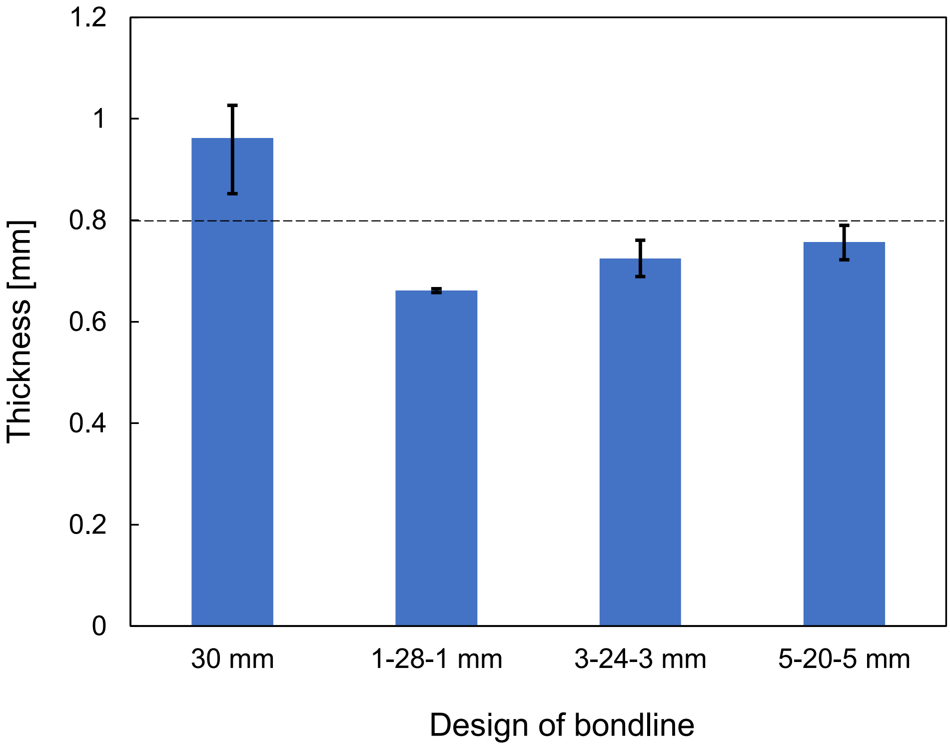

(b)

Fig. 5 Thickness of the bondline obtained from the various tape length for the joint of acrylic plate and aluminum plate (a) and the joint of aluminum plates (b)

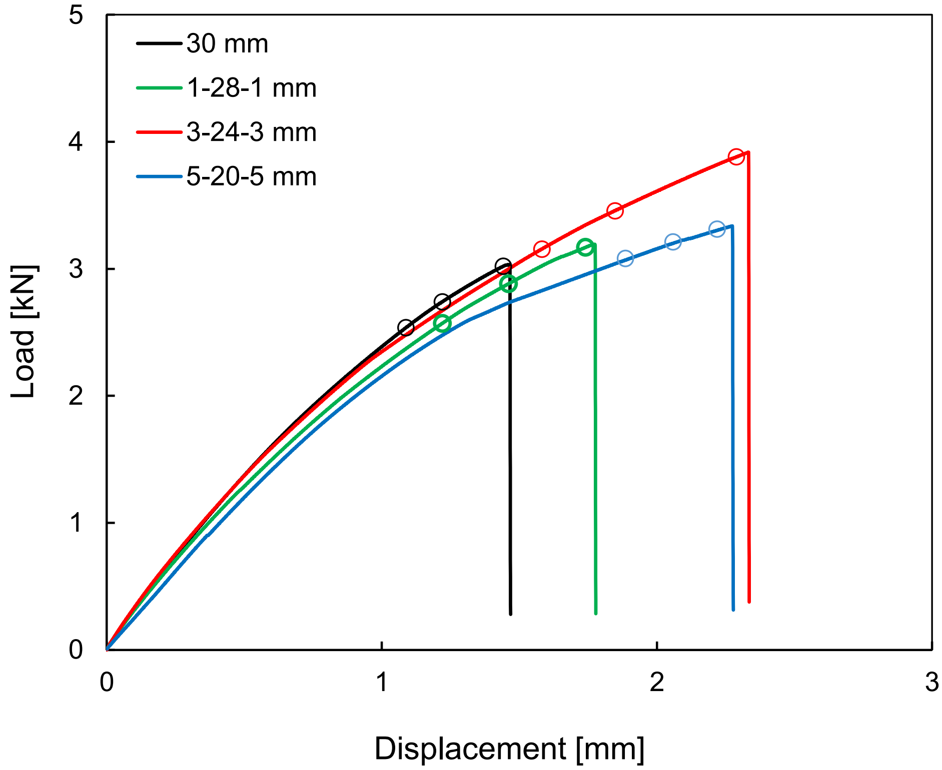

(a)

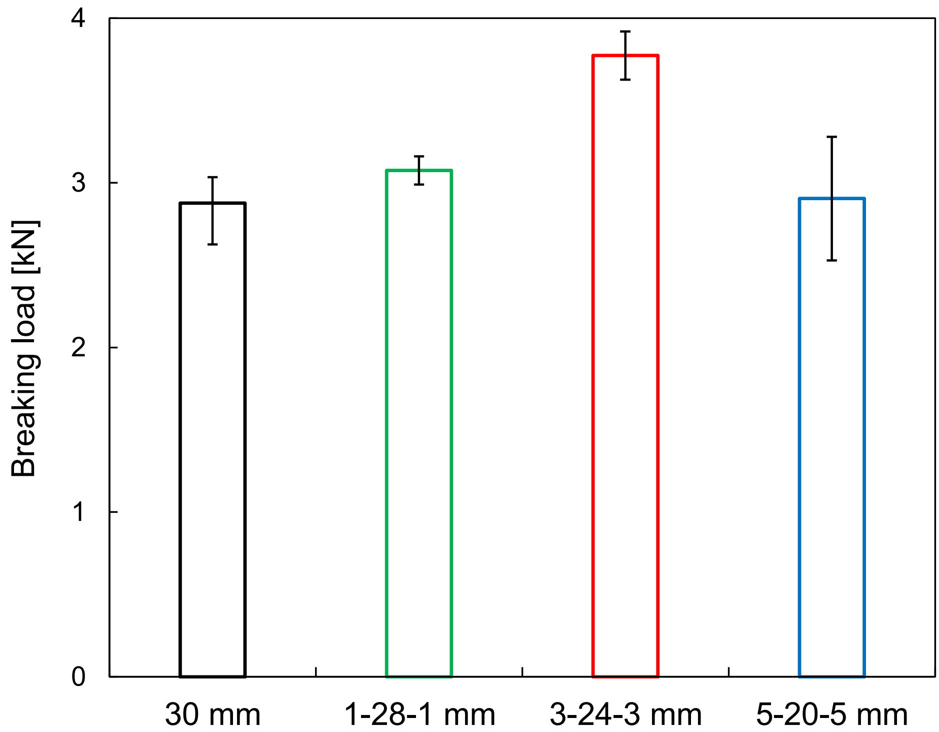

(b)

Fig. 6 Tensile shear test of the joint of acrylic plate and aluminum plate with various tape length

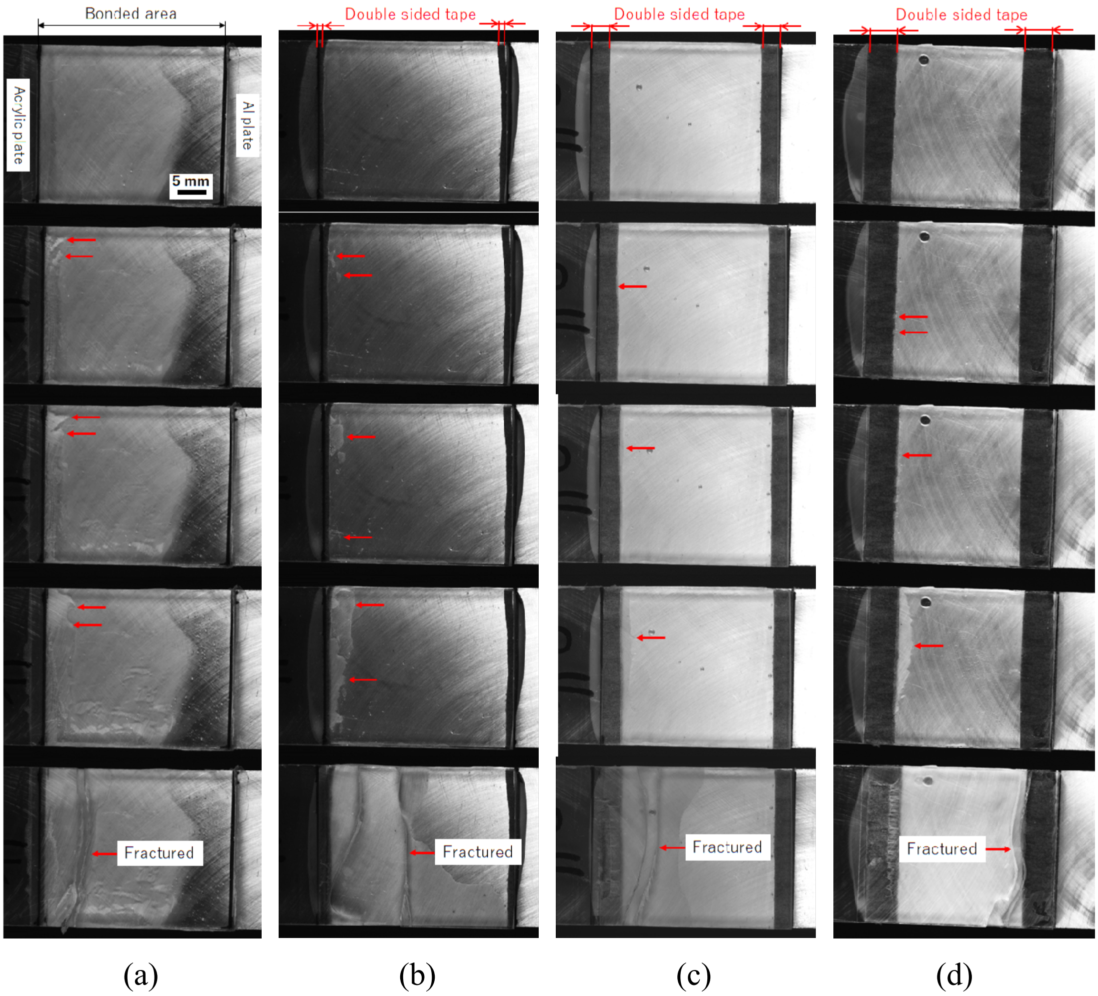

Fig. 7 Observation of bonded-area through acrylic plate for the bond-line of 30 mm (a), and the replacement of both ends by double-sided tape with 1 mm (b), 3 mm (c) and 5 mm (d) tape

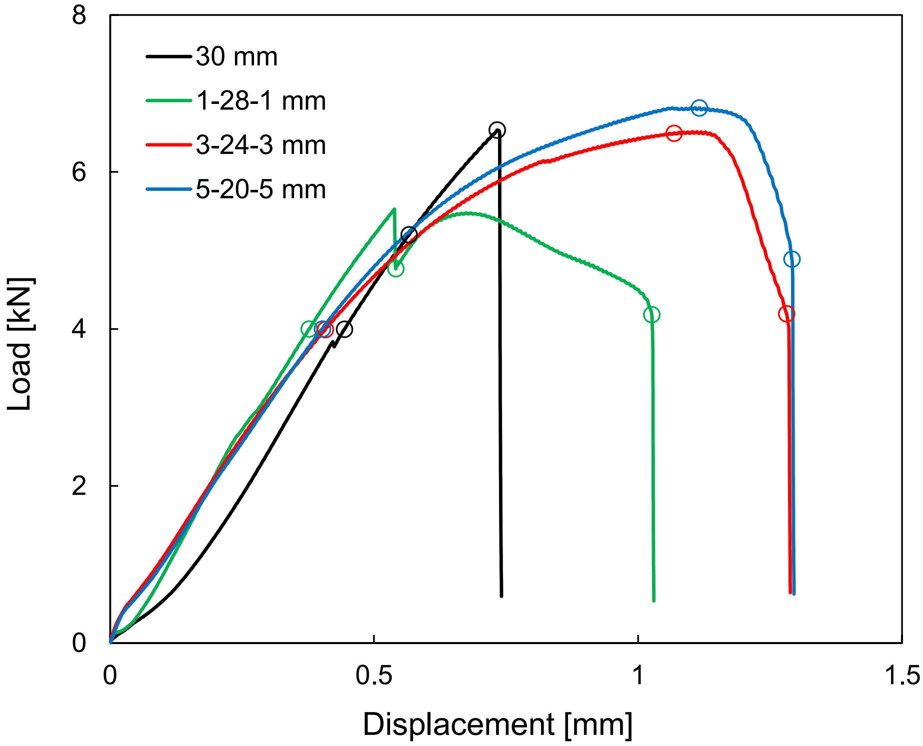

(a)

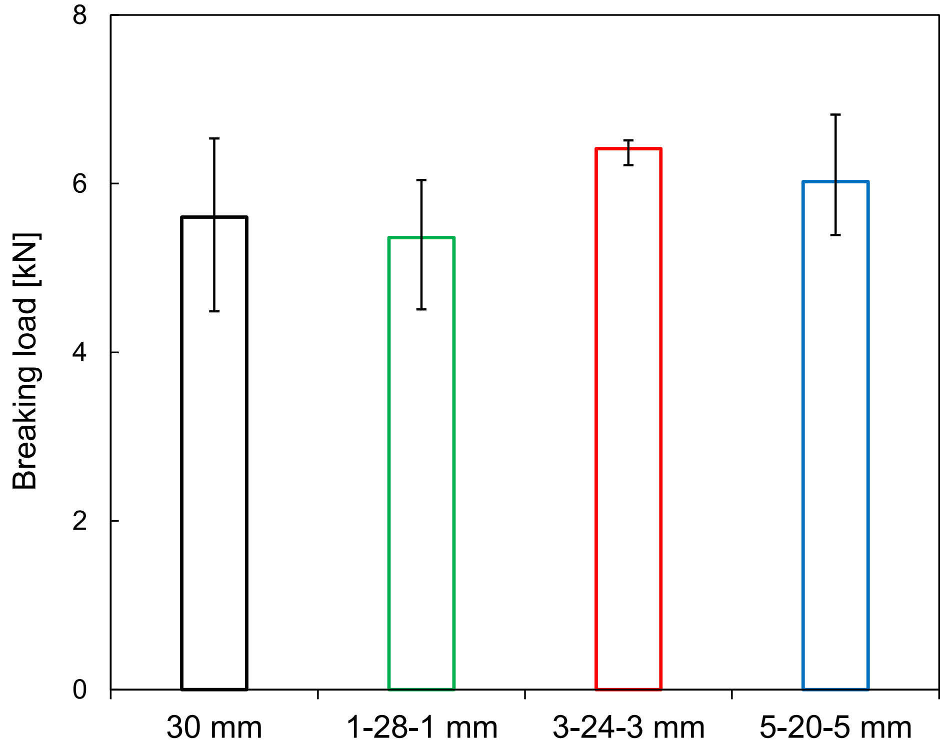

(b)

Fig. 8 Tensile shear test of the joint of aluminum plates with various tape length

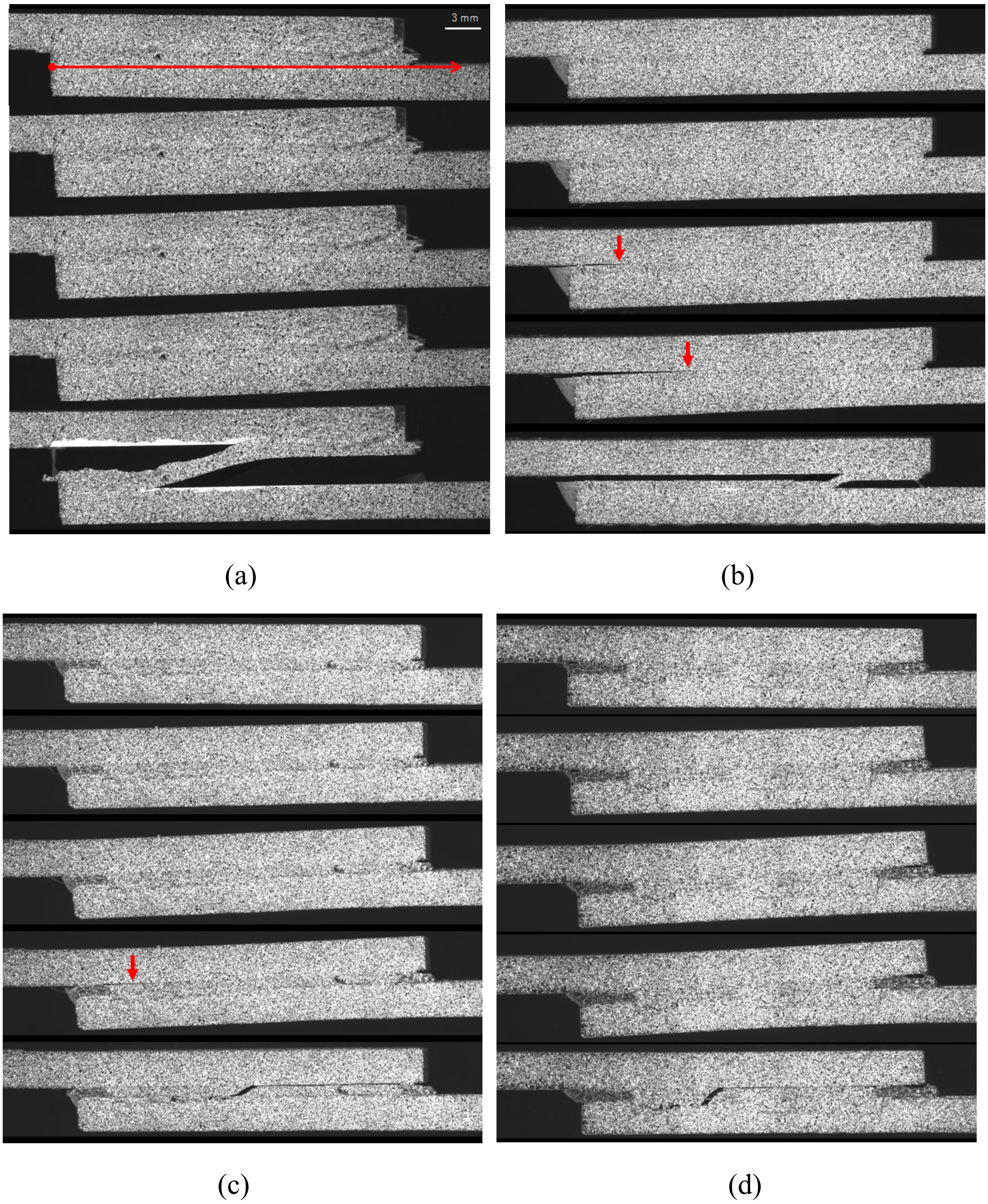

Fig. 9 Images captured by a high-speed camera at the progressive deformations indicated by the circles in Fig. 8 obtained from the bond-line of 30 mm (a), and the replacement of both ends by double-sided tape with 1 mm (b), 3 mm (c) and 5 mm (d)

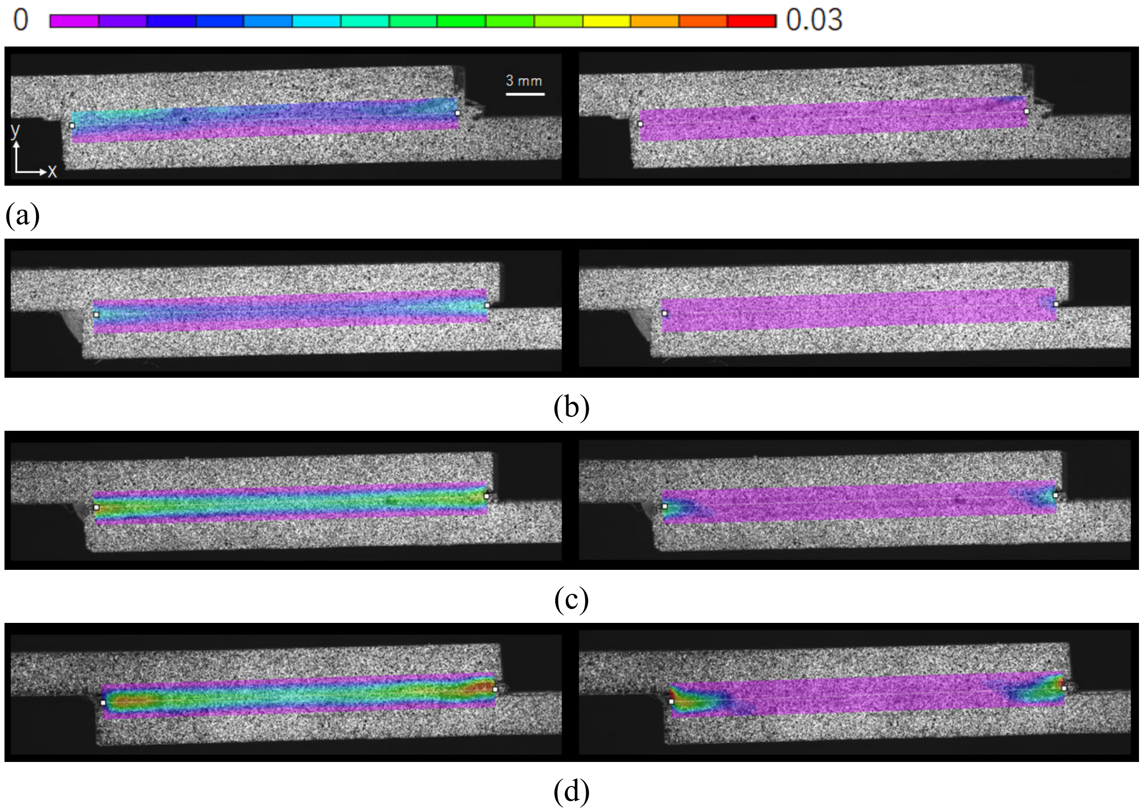

Fig. 10 Distribution of shear (left) and normal (right) strains at the tensile load of 4 kN obtained by digital image correlation method for the bond-line of 30 mm (a), and the replacement of both ends by double-sided tape with 1 mm (b), 3 mm (c) and 5 mm (d)

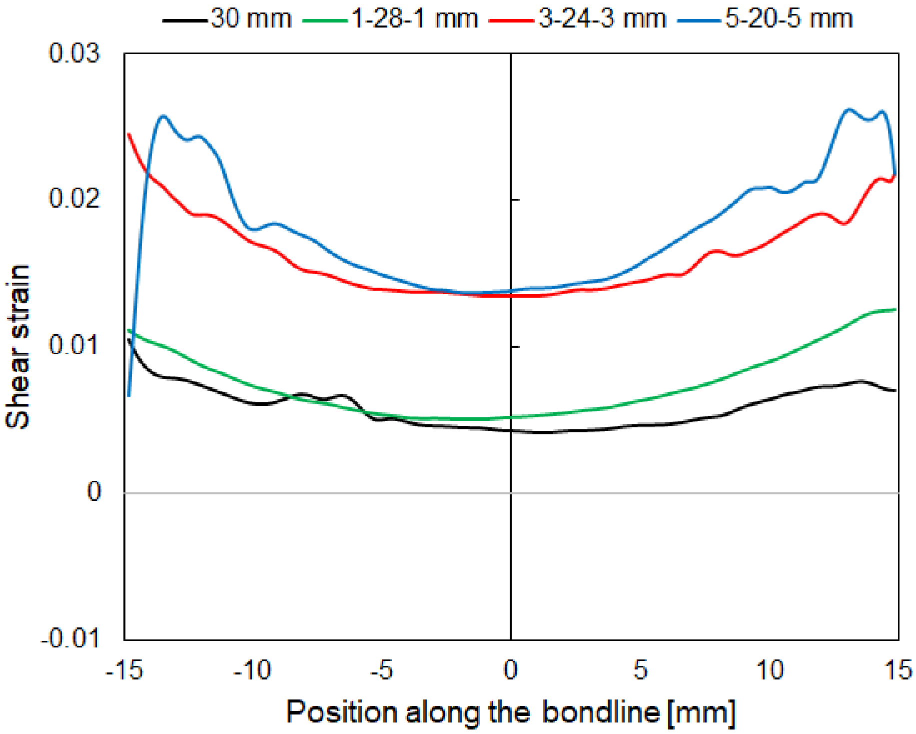

(a)

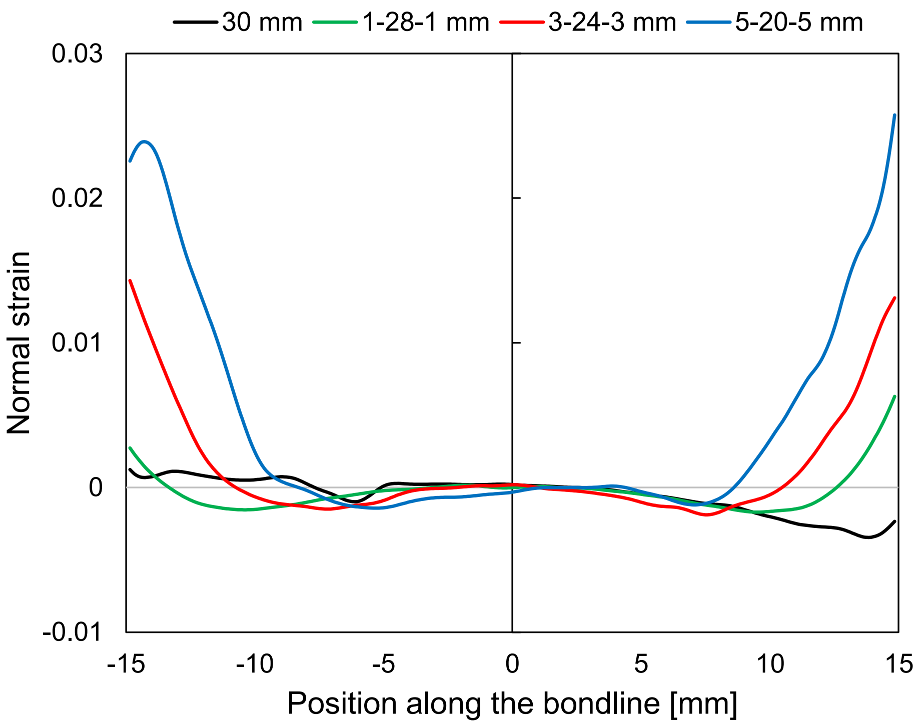

(b)

Fig. 11 Distribution of shear (a) and normal (b) strains in the middle of the adhesive layer at the tensile load of 4 kN for the bond-line of 30 mm (a), and the replacement of both ends by double-sided tape with 1 mm (b), 3 mm (c) and 5 mm (d)

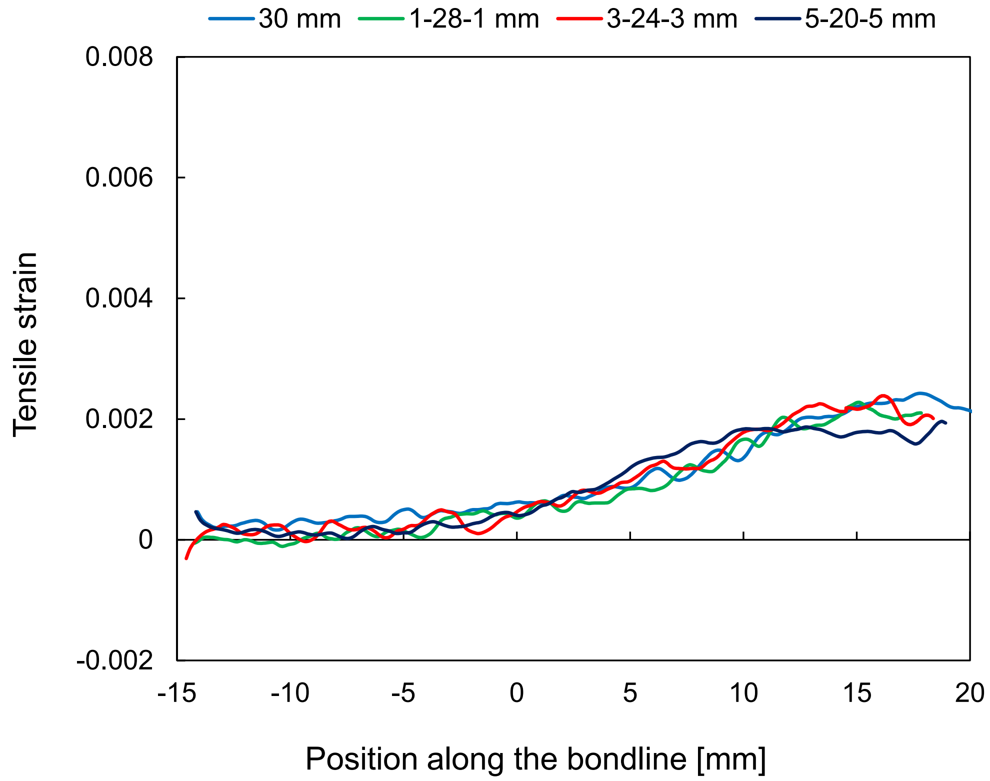

(a)

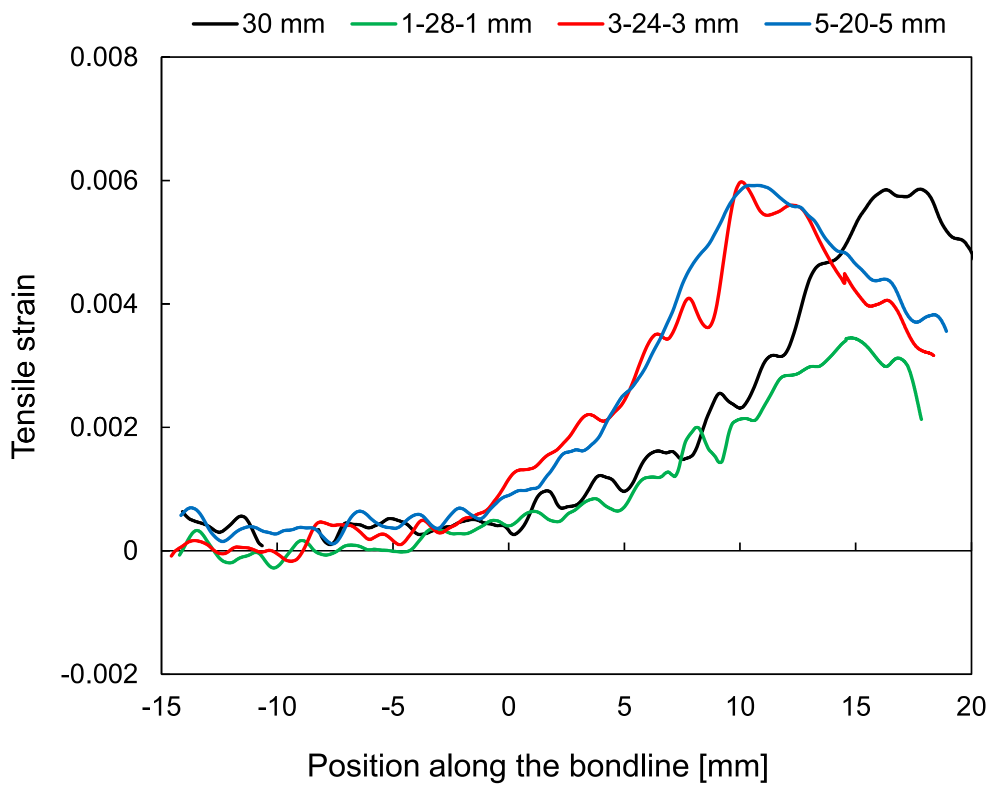

(b)

Fig. 12 Distribution of tensile strains in the aluminum plate along the interface at the tensile load of 4 kN f (a), and at the maximum loads (b)